Relative Isomer Abundance of Fullerenes and Carbon Nanotubes Correlates with Kinetic Stability

A. S. Fedorov,[1,*] D. A. Fedorov,[1] A. A. Kuzubov,[2] P. V. Avramov,[2,3] Y. Nishimura,[4] S. Irle,[4] and Henryk A. Witek[5]

[1]*Kirensky Institute of Physics, Akademgorodok 50, Krasnoyarsk, 660036, Russia*
[2]*Siberian Federal University, av. Svobodny 79, Krasnoyarsk, 660041, Russia*
[3]*Advanced Science Research Center, Japan Atomic Energy Agency, 2-4 Shirakata Shirane, Tokai-mura, Naka-gun, Ibaraki-ken 319-1195, Japan*
[4]*Institute for Advanced Research and Department of Chemistry, Furo-cho, Chikusa-ku, Nagoya 464-8602, Japan*
[5]*Department of Applied Chemistry and Institute of Molecular Science, National Chiao Tung University, Hsinchu 30010, Taiwan*

(Received 2 March 2011; published 20 October 2011)

A methodology to evaluate the kinetic stability of carbon nanostructures is presented based on the assumption of the independent and random nature of thermal vibrations. The kinetic stability is directly correlated to the cleavage probability for the weakest bond of a given nanostructure. The application of the presented method to fullerenes and carbon nanotubes yields clear correlation to their experimentally observed relative isomer abundances. The general and simple formulation of the method ensures its applicability to other nanostructures for which formation is controlled by kinetic factors.

DOI: 10.1103/PhysRevLett.107.175506 PACS numbers: 81.05.ub, 63.22.−m, 65.80.−g

Although fullerenes have been known for over two decades [1], surprisingly, their formation mechanism is still a matter of considerable debate. Many models were proposed to explain relative cage abundances, but all of them suffer from severe drawbacks. In the early models [2,3], the fullerene cage was thought to be formed by the sequential addition of small carbon clusters into quasi-icosahedral spiral shells, in analogy to a growing snail or snowball. These spiroids were indeed shown to exist as intermediate species during the irradiation of carbon soot by an electron beam [4]. However, the snowball mechanism cannot explain the high abundance of $I_h - C_{60}$ and $D_{5h} - C_{70}$. Smalley stressed therefore the importance of realizing a maximum ratio of isolated pentagons over hexagons in the fullerene cage, and proposed the pentagon road [5]. In this mechanism, C_2 units are added to the growing bowl-shaped structure in such a way that alternating hexagons and pentagons are formed. Moreover, it had become clear that abutting pentagons are energetically penalized, leading to the formulation of the isolated pentagon rule (IPR). Since $I_h - C_{60}$ and $D_{5h} - C_{70}$ are the first and second smallest fullerenes obeying IPR, and simultaneously possess the highest and second-highest possible ratio of isolated pentagons over hexagons, their high abundance was explained in this way. However, there was no experimental or theoretical verification of the central tenet of the pentagon road, namely, whether it really is necessary to achieve a maximum ratio of isolated pentagons over hexagons. Further, it was not clear how the C_2 units were directed in their final positions during the high-temperature synthesis. The ring stacking mechanism by Achiba and Wakabayashi [6] proposed that macrocyclic C_n rings stack in precisely determined sequences, leading to C_{60} and C_{70} in ring condensation reactions following two related but different stacking sequences. A variety of other self-assembly mechanisms have been proposed; see, for example, the review by Goroff [7]. Curl *et al.* proposed early on that the surprising abundance of C_{60} and C_{70} has a kinetic origin [8] and recently suggested that the fullerene cage sizes may change during the formation [9]. Recent experimental evidence [10,11] points to initial formation of giant fullerenes C_n with $n > 80$, followed by cage shrinking down to the size of C_{60} due to carbon elimination. In the latter experiment [11], the authors provided the first visual confirmation of the shrink-wrap mechanism [5,12] and its generalization to the shrinking hot giant (SHG) road of fullerene formation [13–15]. Here, hot giant refers to the concept that fullerenes are first formed as vibrationally excited and structurally defective giant fullerenes (GFs), which are subsequently shrinking (referred to as shrink-wrap) by removal of carbon species (mostly C_2) from fullerene cages to sizes as small as the C_{60} molecule. The shrinking process that is part of the SHG road seems obvious when comparing fullerene cage size distribution before [10] and after [1] annealing. The important role of C_2 cluster evaporation during laser shrink wrapping was demonstrated in [16].

To summarize, all available data seem to indicate that large carbon clusters (GFs and possibly others) can self-assemble in hot carbon plasma or vapor, and that the clusters shrink in size due to C_2 evaporation when the carbon vapor plume expands.

We wish to point out here that the often assumed proportionality between the yield of species and their Boltzmann distribution $\exp(-E_{\mathrm{bind}}/kT)$ value, where E_{bind} is the binding energy per atom and T is the synthesis temperature, does not apply to the fullerene synthesis process. This conclusion follows from the observation

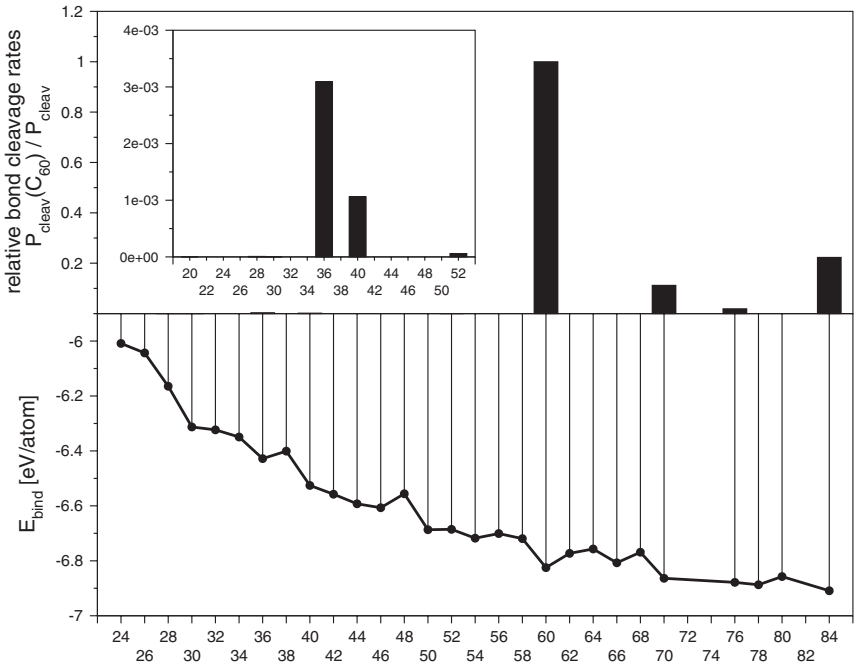

FIG. 1. Calculated relative kinetic stability (upper part) and binding energy from [17] (bottom part) for different fullerenes.

that larger fullerenes have a larger value of E_{bind} as shown in the lower panel of Fig. 1 [17], while experiments demonstrate that larger fullerenes are less abundant than smaller ones, see Table I. This means that the fullerene synthesis is not an equilibrium process and that it is necessary to invoke kinetic stability (KS) arguments to explain the experimentally observed cage size distribution after annealing [8]. In this work we propose a methodology for the estimation of KS of fullerene cages. We show that KS values for different fullerenes, see again Fig. 1, are consistent with the SHG road of fullerene formation [13–15], and it is also applicable for estimating the yield of related carbon nanostructures, e.g., single-walled carbon nanotubes (SWCNTs).

For that equilibrium geometries of selected fullerenes and SWCNTs were computed with density functional theory (DFT) [19,20] using the PBE functional [21,22] in combination with plane wave basis set and ultrasoft Vanderbilt pseudopotentials [23] as implemented in the VASP 4.6 code [24,25]. For SWCNT calculations, the integration over the first Brillouin zone (BZ) was carried out using 4 k points, located along the CNT axis and chosen by the Monkhorst-Pack k-point sampling algorithm [26]. The geometry optimization was carried out with the force convergence criterion of 0.05 eV/Å. The kinetic energy cutoff was equal to 287 eV. Harmonic vibrational frequencies and eigenmodes were calculated using numerical differentiation of atomic forces. The phonon curves were determined with the frozen phonon method [27] using (0,0,0) and $(0,0,\pi/a)$ BZ k points.

Our kinetic stability model is based on the assumption that a cluster consisting of N atoms can be treated as a collection of $3(N-2)$ modes of uncoupled harmonic oscillators. At that six modes corresponded to translations and rotations of the cluster are inessential for consideration of the cluster thermal vibrations, so we can omit them. We express the time-dependent coordinate vector of atom n as

$$\vec{R}(n,t) = \vec{R}_0(n) + \sum_{k=1}^{3(N-2)} \vec{X}_k(n) \exp(i(\omega_k t + \phi_k)), \quad (1)$$

where $\vec{R}_0(n)$ denotes atomic coordinates at equilibrium geometry, $\vec{X}_k(n)$ denotes the portion of the kth vibrational eigenvector $\vec{X}_k$ referring to the atom n, and ϕ_k is the corresponding vibrational phase. In the harmonic approximation the average kinetic and potential energies of a mode k are equal as

$$E_{\mathrm{pot}} = E_{\mathrm{kin}} = \frac{m_k}{2} \sum_{n=1}^{N} |\dot{\vec{X}}_k(n)|^2 = \frac{m_k}{2} \omega_i^2 \vec{X}_k^2, \quad (2)$$

where m_k is the reduced mass. Taking into account thermal equilibrium with environment, $E_{\mathrm{total}} = E_{\mathrm{pot}} + E_{\mathrm{kin}} = kT$, yields the relationship between the temperature and the magnitude of a vibration k as

TABLE I. Relative yield of some fullerene isomers produced using the arc discharge method of Krätschmer. Data taken from [18].

C_{60}/soot ratio	$\approx 10\%$
C_{70}/C_{60}ratio	$\approx 10\%$
$C_n (n = 74, 76, 78, 80, 82, 84, \text{etc})/C_{60}$	$<1\%$
C_{36}/C_{60}	$\approx 1-2\%$

$$|\vec{X}_k| = \sqrt{\frac{kT}{m_k \omega_k^2}}. \quad (3)$$

Time-dependent displacements of atoms n and m can be computed using Eq. (1) as

$$\Delta\vec{R}(n, m, t) = (\vec{R}_0(n) - \vec{R}_0(m)) + \sum_{k=1}^{3(N-2)} (\vec{X}_k(n) - \vec{X}_k(m)) \exp(i(\omega_k t + \phi_k)). \quad (4)$$

A projection of the displacement $\Delta\vec{R}(n, m, t)$ on the equilibrium bond direction can be written as

$$\Delta R(n, m, t) = |\Delta\vec{R}(n, m, t)| \times \cos[\Delta\vec{R}(n, m, t), \times (\vec{R}_0(n) - \vec{R}_0(m))]. \quad (5)$$

According to the central limit theorem in probability theory, the average $\bar{X} = \frac{1}{n}\langle\sum_{k=1}^{n} X_k\rangle$ of variables X_k converges to the normal distribution function when n approaches infinity. Thus, using the central limit theorem and Eqs. (2)–(5), it is possible to calculate the distribution of the projected displacements between all pairs of adjacent atoms. Assuming that a chemical bond between atoms n and m is broken if $\Delta R(n, m, t) \geq X_{\max}$, the bond breaking probability $P(\Delta R(n, m, t) \geq X_{\max})$ is given by

$$P\left(\sum_{i=1}^{3(N-2)} \frac{|\vec{X}_i(n) - \vec{X}_i(m)|e^{i(\omega_i t+\phi_i)}}{\sigma_i} > X_{\max}\right) = \frac{1}{\sqrt{2\pi}s_n} \int_{X_{\max}}^{\infty} \exp\left(-\frac{u^2}{2}\right)du, \quad (6)$$

where the expression on the right-hand side of Eq. (6) is the normal cumulative distribution function and the total variance s_n is defined by $s_n^2 = \sum_{i=1}^{n} \sigma_i^2$ with σ_i being the variance of $\vec{X}_i$. We adopted the value $X_{\max} = 1.95$ Å as the critical distance of C–C bond cleavage. The stability data obtained from our model at $T = 3000$ K are in close agreement with experimental findings (upper panel of Fig. 1). An analysis of the data in Table II shows that the inverse of the calculated fullerene cleavage probabilities qualitatively agrees with the isomer abundance measured experimentally. The C_{60}, C_{70}, and C_{84} fullerenes have the smallest bond breaking rates and simultaneously reveal maximal yield in plasma synthesis. Furthermore, the experimental yield of the $C_{84}(D_{2d})$ fullerene is 1.5 times higher than that of $C_{76}(D_2)$ [28], as is qualitatively confirmed by our cleavage probabilities. On the other hand, the experimental yield of the $C_{36} - D_{6h}$ from [18] is higher than predicted by our calculated kinetic stability. The discrepancy can be explained by the strong sensitivity of C_{36} and other fullerene cage abundances to the experimental and separation conditions, as the authors of [18] mention in their work.

We note that isomers of the same cage size may have dramatically different bond cleavage probabilities as indicated by the $C_{60-}I_h$ with and without a Stone-Wales (SW) defect: 1.03×10^{-13} and 8.54×10^{-15}, respectively. The latter comparison shows that the SW defect leads to high cleavage probability, as assumed in the prevailing shrink-wrap mechanism [12]. The application of our KS model to SWCNTs (see Table III) demonstrates inverse dependence of P_{cleav} on the nanotube diameter d, which is in qualitative agreement with experimental findings for SWCNT abundance, see [29].

Also we investigated the role of the bond network environment around the weakest bond for the destruction rate of the P_{cleav} for $C_{30} - D_{5h}$ cage. To this end we analyzed the dependence of P_{cleav} on the number of actually vibrating atoms by performing calculations where all atoms of the cage were divided in seven separable tiers. The first tier contained the two atoms defining the weakest bond, tier 2 contained all the directly bound neighbors of atoms in tier 1, etc. Dependence of the destruction rate on the

TABLE II. Fullerenes bond cleavage probabilities $P_{\text{cleav}}(\text{sec}^{-1})$, relative bond cleavage rates $P_{\text{cleav}}(C_{60})/P_{\text{cleav}}$ from the kinetic and thermodynamic* [17] stability methods, and DFT binding energies E_{bind} (eV/bond).

Struct.	Symmetry	P_{cleav}	$\frac{P_{\text{cleav}}(C_{60})}{P_{\text{cleav}}}$	$\frac{P_{\text{cleav}}(C_{60})}{P_{\text{cleav}}}$*	E_{bind}
C_{84}	D_{2d}	$3.84E-14$	0.223	1.368	−5.933
C_{76}	D_2	$4.55E-13$	0.019	1.231	−5.912
C_{70}	D_{5h}	$7.57E-14$	0.112	1.163	−5.912
C_{60}	I_h	$8.54E-15$	1	1	−5.887
C_{60}	I_h-SW	$1.03E-13$	0.083	···	−5.870
C_{52}	C_{3v}	$1.50E-10$	$5.69E-05$	···	−5.736
C_{40}	T_d	$8.05E-12$	$1.06E-03$	0.259	−5.700
C_{36}	D_{6h}	$2.76E-12$	$3.09E-03$	0.188	−5.685
C_{36}	C_1	$1.88E-10$	$4.54E-05$	···	−5.654
C_{30}	D_{5h}	$2.62E-08$	$3.26E-07$	0.138	−5.548
C_{30}	C_{2v}	$1.92E-11$	$4.44E-04$	···	−5.592
C_{28}	D_2	$1.02E-09$	$8.37E-06$	···	−5.529
C_{20}	I_h	$1.92E-06$	$4.45E-09$	···	−5.379

TABLE III. Bond cleavage probabilities $P_{\text{cleav}}(\text{sec}^{-1})$, relative bond cleavage rates $P_{\text{cleav}}(C_{60})/P_{\text{cleav}}$, and DFT binding energies E_{bind} (eV/bond) for selected SWCNTs.

Structure	Diameter d	P_{cleav}	$\frac{P_{\text{cleav}}(C_{60})}{P_{\text{cleav}}}$	E_{bind}
CNT(5,0)	3.91	$1.66E-13$	0.051	−5.794
CNT(6,0)	4.69	$4.99E-15$	1.711	−5.890
CNT(8,0)	6.26	$3.33E-16$	25.64	−6.000
CNT(5,5)	6.77	$1.11E-16$	76.94	−6.022

number of vibrating atoms in some successive tiers, given in Table IV, show that for reproducing the correct magnitude of P_{cleav} one has to allow practically all atoms in a given nanostructure to vibrate. This analysis shows that the bond breaking process is a global phenomenon involving practically all atoms of the structure, even if the destruction process have a quite local character. Also an analysis of weakest bond length for all investigated fullerenes shows that this bond is not necessarily the longest bond in the fullerene, especially for small fullerenes, although it is among the longer bonds. Figures of weakest bonds in selected fullerenes are given in the supplementary material [30]. The presented KS model, based on determination of the cleavage probability for the weakest bond of a given nanostructure due to thermal vibrations, has been successfully applied to explain the experimentally observed isomer abundance of fullerenes and single-walled nanotubes in carbon soot. It was found that C_{60}, C_{70} and C_{84} have the smallest bond breaking rates, which inversely correlates with their observed abundance in high-temperature synthesis. Despite of larger thermodynamic stability of C_{70} over C_{60}, its KS predicted by our model is 1 order of magnitude smaller. Thus, for the first time in the history of fullerene research the predominance of C_{60} over C_{70} in the carbon soot could be rationalized. Our model was also successfully applied to SWCNTs, where inverse correlation of KS with the tube diameter was found. Note, however, that for SWCNTs, in contrast to fullerenes, the kinetic and thermodynamic stabilities follow the same trends.

TABLE IV. Dependence of destruction probability $P_{\text{cleav}}(\text{sec}^{-1})$ on the number of vibrating atoms belonged to tier series in the C_{30} D_{5h} fullerene.

Tier	Number of vibrating atoms	P_{destr}
1	2	$5.47E-13$
2	6	$9.09E-13$
3	12	$3.15E-12$
4	18	$5.89E-12$
5	24	$1.05E-10$
6	29	$2.55E-8$
7	30	$2.62E-8$

S. I, P. V. A, and A. S. F gratefully acknowledge generous hospitality during their visits to Krasnoyarsk (S. I) and Fukui Institute for Fundamental Chemistry in Kyoto and Nagoya University (P. V. A and A. S. F) under support of the joint JSPS-RFBR travel grant 09-02-92107. This work was partially supported by National Science Council (grants NSC96-2113-M009-022-MY3 and NSC96-2113-M009-011-MY3) and Ministry of Education of Taiwan (MOE-ATU project), as well as by the JAEA Research fellowship (P. V. A). We thank the Institute of Computer Modeling (Siberian Division of RAS) and the Joint Supercomputer Center RAS for opportunity to use cluster computers for performing all calculations.

*alex99@iph.krasn.ru

[1] H. W. Kroto, J. R. Heath, S. C. O'Brien, R. F. Curl, and R. E. Smalley, Nature (London) **318**, 162 (1985).
[2] H. W. Kroto and K. McKay, Nature (London) **331**, 328 (1988).
[3] H. W. Kroto, Science **242**, 1139 (1988).
[4] E. Osawa, J. Phys. Chem. **106**, 7135 (2002).
[5] R. E. Smalley, Acc. Chem. Res. **25**, 98 (1992).
[6] T. Wakabayashi, P. Shiromaru, K. Kikuchi, and Y. Achiba, Chem. Phys. Lett. **201**, 470 (1993).
[7] N. S. Goroff, Acc. Chem. Res. **29**, 77 (1996).
[8] R. F. Curl and R. C. Haddon, Phil. Trans. R. Soc. A **343**, 19 (1993).
[9] R. F. Curl, M.-K. Lee, and G. E. Scuseria, J. Phys. Chem. A **112**, 11 951 (2008).
[10] M. Bogana *et al.*, New J. Phys. **7**, 81 (2005).
[11] J. Y. Huang, F. Ding, K. Jiao, and B. I. Yakobson, Phys. Rev. Lett. **99**, 175503 (2007).
[12] S. C. O'Brien, J. R. Heath, R. F. Curl, and R. E. Smalley, J. Chem. Phys. **88**, 220 (1988).
[13] S. Irle, G. Zheng, M. Elstner, and K. Morokuma, Nano Lett. **3**, 1657 (2003).
[14] G. Zheng, S. Irle, and K. Morokuma, J. Chem. Phys. **122**, 014708 (2005).
[15] S. Irle, G. Zheng, Z. Wang, and K. Morokuma, J. Phys. Chem. **110**, 14 531 (2006).
[16] G. Ulmer, E. E. B. Campbell, R. Kuhnle, H. G. Busmann, and I. V. Hertel, Chem. Phys. Lett. **182**, 114 (1991).
[17] F. N. Tomilin, P. V. Avramov, S. A. Varganov, A. A. Kuzubov, and S. G. Ovchinnikov, Fiz. Tverd. Tela (S. Peterburg) **43**, 936 (2001) [Phys. Solid State **43**, 973 (2001)].
[18] C. Piskoti, J. Yargen, and A. Zettl, Nature (London) **393**, 771 (1998).
[19] P. Hohenberg and W. Kohn, Phys. Rev. **136**, B864 (1964).
[20] W. Kohn and L. J. Sham, Phys. Rev. **140**, A1133 (1965).
[21] J. P. Perdew, K. Burke, and M. Ernzerhof, Phys. Rev. Lett. **77**, 3865 (1996).
[22] J. P. Perdew, K. Burke, and M. Ernzerhof, Phys. Rev. Lett. **78**, 1396 (1997).
[23] D. Vanderbilt, Phys. Rev. B **41**, 7892 (1990).

[24] G. Kresse and J. Furthmüller, Comput. Mater. Sci. **6**, 15 (1996).
[25] G. Kresse and J. Furthmüller, Phys. Rev. B **54**, 11 169 (1996).
[26] H. J. Monkhorst and J. D. Pack, Phys. Rev. B **13**, 5188 (1976).
[27] J. Kürti, G. Kresse, and H. Kuzmany, Phys. Rev. B **58**, R8869 (1998).
[28] K. Tohji, A. Paul, L. Moro, R. Malhotra, D. C. Lorents, and R. S. Ruoff, J. Phys. Chem. **99**, 17 785 (1995).
[29] F. Simon, A. Kukovecz, C. Kramberger, R. Pfeiffer, F. Hasi, H. Kuzmany, and H. Kataura, Phys. Rev. B **71**, 165439 (2005).
[30] See Supplemental Material at http://link.aps.org/supplemental/10.1103/PhysRevLett.107.175506 for details.